X-692-71-385
PREPRINT

THE IMP-H ION COMPOSITION EXPERIMENT

M. H. ACUNA
K. W. OGILVIE

SEPTEMBER 1971

GSFC
GODDARD SPACE FLIGHT CENTER
GREENBELT, MARYLAND

THE IMP-H ION COMPOSITION EXPERIMENT

by

M. H. Acuna
and
K. W. Ogilvie

Laboratory for Extraterrestrial Physics
NASA-Goddard Space Flight Center
Greenbelt, Maryland 20771

September 1971

Introduction

During the past few years, a number of experiments[1,2,3,4] have been successfully flown aboard satellites and space probes for the purpose of studying the composition, properties and temporal behavior of the interplanetary plasma. As our knowledge of the interplanetary medium has increased, these experiments have become more sophisticated and specific in purpose.

The composition of the plasma has been studied using energy-per-unit-charge spectra[5,5a] and using energy-per-unit charge and velocity analysis[6,6a]. The results show a variable proportion of H_e, with the H_e/H ratio between 0.01 and 0.20. The presence of heavier ions has been demonstrated and the O/H_e ratio determined.

This paper describes a compact mass-energy spectrometer to be flown aboard the IMP-H spacecraft. The scientific aims are the determination of the relative and absolute fluxes of $_4H_e^{++}$, $_4H_e^{+}$, $O^{(6+)}$ and $O^{(7+)}$, and $_3H_e^{++}$. The successful realization of these aims would result in at least the following interesting studies.

1). A study of the variation of $_4H_e^{++}$ both on the long term, as a function of time in the solar cycle, and on the short time scale following interplanetary shocks[7].

2). A series of determinations of the proportion of Oxygen in the solar wind, and its variation. The variation of Oxygen in post-shock gases will help to decide whether these gases represent the 'piston' driving the shocks.

3). A study of the flux of $_4H_e^{+}$ in the interplanetary medium and sheath. These ions cannot exist in the corona[8], and therefore if detected must be of relatively local origin. They may come from the ionization

of interstellar helium, or from the ionization of terrestrial helium. Their energy spectrum could decide this question.

4). The ratio $_3H_e^{++}/_4H_e^{++}$ is sensitive to the acceleration process in the lower solar corona[9]. Knowledge of variations in this density ratio as a function of solar activity are essential to an understanding of the acceleration process. A successful theory of the fractionation of elements in the lower corona must be able to predict this variation, and the usefullness of these particular ions lie in the large percentage difference between the values of m/z which characterize them.

5). The large circular orbit of IMP H is very suitable for studying the proportion of H_e^+ in the sheath downstream from the earth. H_e^+ ions formed in the sheath, and accelerated in the turbulent sheath plasma, form an interesting subject for research with this instrument.

6). In addition to the quantities described above it will be possible to obtain the plasma bulk speed and the temperature and density of $_4H_e^{++}$. These quantities will be averages characteristic of the time of measurement, 37.5 seconds to aquire data for a determination, with determinations spaced by a time of 10 minutes. Full investigation of the variation of the temperature of H_e in the solar wind has not so far been carried out.

Experiment description

A photograph of the experiment package is shown in Figure 1. It is contained in a standard IMP series housing and weighs 7.8 pounds. Total power consumption is 1.4 watts:

The experiment consists of four principal parts:

1) An ion optics section

2) A detector section

3) Deflection voltage supplies

4) Signal conditioners and command logic.

1. Ion Optics Section

A schematic representation of the ion optics section is shown in Figure 2. It consists of a cylindrical curved plate electrostatic analyzer and a crossed-field velocity selector or Wein filter. Its basic design criteria have been described by Ogilvie et al.[10] and somewhat similar versions have been flown previously aboard the IMP series of satellites. Only minor modifications have been incorporated in the present instrument in order to improve mass resolution and spatial response characteristics. Plasma ions with a given energy-per-unit charge will pass paraxially through the electrostatic analyzer if the relation

$$(mv^2/zq) = 2\ (V_c R/\Delta R) \qquad (1)$$

is satisfied. Here m is the ion mass, v its velocity, zq its charge, $\pm V_c$ is the potential applied to the plates, R and ΔR are their mean radius and separation respectively, and $(\Delta R/R)^2$ is neglected. For the instrument under consideration the energy passband is 4%, corresponding to a velocity passband of 2%. The crossed-field velocity selector,

selects ions with a velocity satisfying the no net force relation

$$\underset{\sim}{E} + \frac{1}{C}(\underset{\sim}{V} \times \underset{\sim}{B}) = 0 \qquad (2)$$

where $\underset{\sim}{E}$ is the applied electric field between the plates of the velocity selector and $\underset{\sim}{B}$ the internal magnetic field, (750 gauss).

With a velocity bassband of 2%, the maximum mass per unit charge resolution ($=V/\Delta V$) possible is thus 50. The value achieved in practice is $\sim$30, the discrepancy being attributable to the large angular aperture of the instrument and to penumbral effects in the Wein filter. The principal advantage of this sytem of electrostatic analyzer and short[11] Wein filter is its high transmission and compactness, while the resolution is sufficient for many purposes. It could be improved for other purposes[12,13] by correcting various aberrations.

The measurement scheme is to cause the electrostatic analyzer to sequentially select 30 energy-per-charge intervals, and adjust the potential providing the electrostatic deflection of the Wein filter to pass a given species of ion having that energy per charge. Thus, as four ion species are to be studied, a total of 30x4=120 combinations of potentials is required. The magnetic field is obtained from a pair of ALNICO VIII-B magnets enclosed in a box made of Carpenter 49 alloy, providing a low reluctance return path to minimize stray fields which otherwise would affect magnetic measurements performed on board the spacecraft. Only those ions which satisfy (1) and (2) will pass through the ion optics section into the detector with appreciable intensity.

Figure 3 shows the measurement scheme and the results of a test using the ions $_4H_e^+$ and $_4H_e^{++}(H_2^+)$, and H^+ giving an idea of the resolution and freedom from background obtained. The total field of view of the ion optics is restricted to 10 degrees in elevation and 0.8 degrees

in azimuth by means of a slit system located at the entrance of the electrostatic analyzer. This improves mass and energy resolution and reduces scattering of ions and ultraviolet photons. The limiting particle trajectories are shown in Figure 4.

2. Detectors

The detectors consist of two Spiraltron* electron channel multiplier assemblies (SEM's) which are located immediately behind the exit slit of the velocity selector, and aligned as shown in Figure 2. The construction of each SEM assembly is shown in Figure 5, and it includes a bias resistor and coupling capacitor. A cylindrical sleeve insulated from the multiplier section, joined by epoxy cement to the exit aperture of the multiplier serves as the charge collection electrode. The use of a sleeve instead of a sealed cap, provides means for rapid venting of the interior of the SEM to prevent corona problems associated with partial pressure conditions and the high voltage required for operation. During assembly, the SEM is first coated with a 7.6×10^{-3} to 1.27×10^{-2} cm layer of "Solithane" and then placed in a KEL-F box with appropriate entrance and exit apertures. After component installation and interconnections, the assembly is encapsulated in "Stycast 3050" resin.

The "solithane" coating and the "Stycast" resin are used to match as closely as possible the thermal expansion coefficient of the SEM to that of the support structure. The "solithane" coating, is elastic enough to prevent thermal stresses which would eventually destroy the SEM.

The SEM's operate independently of each other, each providing a 5.5 degree field of view for the ions that pass through the optics section.

*Registered Trademark of the Bendix Corp.

They are operated in the gain saturated mode with a nominal gain of 10^8. The axis of each SEM is tilted approximately 2 degrees from the velocity selector optical axis in order to ensure ions striking the multiplier close to its input end. This prevents broadening of the output pulse height distribution with the consequent loss of counts due to the finite threshold of the discriminator. The multiplier is operated with its input end grounded, and the output end at a high positive potential. Thus the energy available for the first secondary electron emission process is that of the ion itself, and a knowledge of the efficiency of secondary emission, and its variation with incident ion energy becomes of great importance. The ion detection efficiency of channel multipliers has been measured by Burrous et al.[14], Egidi et al.[15] and others. The reported values vary from 40% to 90% for the range of energies of interest and the ionic species to be counted. Additional measurements of the detection efficiency under the particular operating conditions of the instrument will be carried out in the near future. Once the first electron has been produced, the method of operation of the spiraltron and the associated charge-sensitive amplifier ensures that it is counted with unit efficiency.

The spectrometer points directly at the sun when the plasma is being analyzed, hence a light trap has been added to the outside plate of the electrostatic analyzer to minimize the amount of ultraviolet light reflected into the detector section. Furthermore, all surfaces exposed to direct or reflected sunlight are appropriately blackened (using electrically conducting chromium or copper black coatings) for the same purpose. This is particularly important as electron channel multipliers

have extremely high quantum detection efficiency for extreme ultraviolet radiation, (Johnson[16]). The use of the light trap and blackened surfaces reduce the predicted back ground count rate due to UV radiation to less than 1 count every 10 seconds.

The intrinsic background count rate obtainable with SEM's is 2 to 3 counts per minute or less; as the instrumentation's contribution is negligible, extremely small fluxes should be detectable. A programmable power supply provides the high voltage required for operation of the SEM's, and the bias for the charge collection electrode. It can be commanded to give 3000, 3500 or 4000 volts, to compensate for the gain fatigue effects to be expected during extended operation of channel multipliers (This problem is covered in more detail later). The bias voltage for the collection electrode is maintained at +200 volts above the indicated values. Three one bit words corresponding to each operating level, and an analog voltage monitor, provide identification and housekeeping data to the spacecraft encoder.

3. Deflection Voltage Supplies

These supplies provide the two deflection voltages required to satisfy equations (1) and (2), Vc and Vm, for each ionic species and energy range of interest, and the low voltage for the amplifiers, signal conditioners and logic.

The analyzer and Wein filter are operated with equal positive and negative potentials applied to the inside and outside plates respectively. This minimizes the directional effects of fringing fields. The thirty values of potential (steps) provided cover the range of 300 to 6500 ev/z for each species, as shown in Figure 3.

Each of the thirty steps is held for five revolutions of the spacecraft, except for the case of $_4He^{++}$ where the steps need only be held for a single revolution due to the larger flux. Table 1 shows the relative abundances of each ionic species and summarizes the measurement scheme. Each spacecraft revolution takes 1.25 sec; the counting interval is the time required for the spacecraft to rotate 0.8 degrees. The total flux and relative abundances used to calculate Table 1 are those given by Hundhausen[17], and the sensitive area, that of the SEM, is $7.9 \times 10^{-3} cm^2$.

TABLE 1

Ion	Nominal Abundances Ref. to H^+	Spins Step	Expected Counts per cycle
$_4He^{++}$	4.6×10^{-2}	1	240
$_0^{6+,7+}$	1.84×10^{-3}	5	50
$_3He^{++}$	9.2×10^{-6}	5	.25
$_4He^{+}$	1.38×10^{-4}	5	4

As the spin rate of the spacecraft is 0.8 rev/sec., each ionic species requires 187.5 seconds for a complete energy scan, except for $_4He^{++}$ which only requires 37.5 seconds. A complete experiment cycle thus requires 480 spins = 600 seconds.

A step command is derived from a solar sensor signal in the spacecraft which advances the deflection supplies to the next step every 5 revolutions or every revolution, as described above. Corresponding to each step and ionic species respectively, a 6 bit word and a 2-bit word are generated and loaded into the spacecraft data processor for identification purposes.

4. Signal Conditioners and Logic

The instrumentation required to interface with the spacecraft encoder has been kept to a minimum as the latter provides counters and loading logic. The SEM's pulses are fed into two separate charge-sensitive preamplifier-amplifier combinations and two discriminators of conventional design. This arrangement, together with the two detectors, provides a degree of redundancy. The charge sensitivity threshold of each set is 5×10^{-14} coulombs, which is sufficient to insure a life expectancy of over one year at 10^4 counts/sec. for the channel multipliers. This count rate is much higher than the expected rates shown in Table 1; hence, the one year figure is extremely conservative, especially if we take into account that the nominal gain of the SEM's (10^8), has to decrease by a factor of more than 100 before there is any significant loss of data.

The discriminator outputs are shaped into 5 μs pulses and fed to a gate which allows the instrument to operate in two scanning modes, selectable by ground command: a) Normal scan mode: In this mode the gate is controlled by the solar sensor signal which is used to step the deflection supplies, and the output is only active for 90° of rotation of the spacecraft, 45° either side of the solar direction. b) Full scan mode: No gating of the outputs is provided when in this mode, hence the experiment output is active for the full 360° of rotation. The gate outputs interface directly with the spacecraft encoder which provides floating point counters and loading logic for housekeeping and identification bits. This arrangement is necessary as the data readout rates are spin synchronized. The contents of the floating point counters are loaded into the encoder and read out only twice per revolution, during the 3rd and 4th quadrants at the normal 1600 bits/sec. rate. If the readout

and spin rates were out of phase, there would be a considerable loss of data, if the full scan mode were not provided. In addition, under normal operating conditions, this mode allows for the observation and study of plasma features not aligned with the solar direction, and provides redundancy against a failure of logic circuits.

Experiment Tests and Performance

1. Ion Optics Test and Calibration. A schematic representation of the ion optics test set-up is shown in Figure 6. Two types of ion sources can be utilized for calibration purposes: A collision type and a radio frequency ion source. In each case ion beams of known composition and energy are generated and focused into the input aperture of the instrument. The R.F. ion source and its associated energy-velocity selection optics have been described in the literature[10], and it is restricted to operation with hydrogen (H_2^+) which is kinetically equivalent to ${}_4H_e^{++}$. The collision source has no such restriction as it uses emission from a hot filament to ionize selected gases admitted into the system. A set of electrostatic lenses provide extraction potentials and focusing optics for the ions thus generated, but the beam cross section and beam currents obtainable are much smaller than in the case of the R. F. source.

The ion beam generated by the collision source is essentially monoenergetic, in contrast to the R. F. source which generates a beam with wide energy distribution so that the energy width is subsequently determined by the associated energy-velocity selection optics. A typical resolution curve obtained with the instrument is shown in Figure 3, for 960 eV ions from the collision source. It indicates a mass resolution of $m/\Delta m = 33$ for ${}_4H_e^{++}$ which is sufficient to allow observation of O^{6+} ions.

The azimuthal angular response characteristics of the spectrometer are shown in Figure 7, for 3 steps of the deflection supplies corresponding to ${}_4H_e^{++}$. These curves show the integrated response of the instrument to a monoenergetic H_2^+ beam incident upon the entrance aperture and do not specifically show the energy-angle dependence typical of electrostatic analyzers.

Figure 8 shows the elevation angular response (i.e. in a plane containing the spin axis) of the instrument; each peak is due to one of the SEM's looking into the incoming collimated beam from the collision source, as the spectrometer is rotated about the geometrical cross-over point in the ion optics section (Figure 4). The redundancy provided by the use of two SEM's is particular useful. In the event of failure of one unit, the elevation angular response is reduced from 10 to 5.5 degrees and only a small fraction of the data would be lost. In addition, great care was taken to minimize the cross-coupling between multipliers, as if one should become intermittent or vary, undesired pulses would be coupled into the other channel. Typically, the observed cross-coupling is less than 1%.

The measurement of the transmission efficiency of the ion optics section requires a precise determination of the ion-beam current density, that is, its cross section and current. The test set-up shown, incorporates a pair of deflection plates which are used to deflect the incoming beam into a Faraday cup and thus measure the total beam current.

A second Faraday cup, with a 2 mm. diameter opening, was located in place of the input aperture of the instrument to determine the relationship between the currents measured at each location and estimate the beam cross section. As the latter was measured to be much greater than the 2 mm aperture cross section, the current density can be assumed to be constant over this area. Hence we obtain the desired relationship between the current measured at the first Faraday cup and the resulting current density at the input aperture of the instrument. The transmission efficiency measured in this fashion, is essentially 100%, although the

method is sensitive to small variations in alignment between the ion beam and detector axes, as well as to focus adjustments if the collision source is used. The R.F. source, producing a much larger beam cross section and being free of focus effects, yields a better estimate of the incident ion flux. and detector efficiency. The energy pass-band of the analyzers at the beam source is less (1%) than that of the instrument. Thus all the current from the source can be made to enter the instrument.

The spectrometer's output ion flux can be measured with the SEM's, but in such case, the ion detection efficiency of the multipliers must be taken into account.

2. Detectors

In testing the detectors, two types of tests were performed on the spiraltron assemblies: a) Environmental tests and b) gain fatigue tests.

a) Environmental Tests

The environmental tests performed on the assemblies comprised sine and random vibration, shock and extensive thermal cycling to ensure that no differential thermal stresses would develop and damage the units. Of a group of 10 assemblies subjected to 10 temperature cycles of $-50^{\circ}C$ to $+50^{\circ}C$ at $15^{\circ}/HR$ rate with a 3 hour period at $-50^{\circ}C$, only one failure was observed.

b) Gain fatigue tests

Channel multiplier gain fatigue effects have been previously observed and reported in the literature[18, 19, 20], but in general, the data was obtained for curved channel multipliers. In the case of SEM's, little or no such data is available, hence a group of units was subjected to gain fatigue tests to determine the variation of the average gains

as a function of the total number of accumulated counts. Six SEM's and associated charge-sensitive preamplifiers were placed in a small cryosorption, gettered ion pumped vacuum system. Titanium sublimation was used to increase pumping speeds until a pressure of 5×10^{-7} torr was achieved and maintained for the duration of the test. Two Ni63 radioactive sources provided the excitation for the SEM's, and the average count rate was adjusted to 10^4 counts/sec. This rate varied somewhat during the test, as approximately 10% of the counts were due to the ion pump. The construction of 5 of the SEM's was similar to that of the ones used in the assemblies, (Figure 5), the remaining unit being an actual flight assembly. The flight SEM assembly had been already screened by the manufacturer for high gain and initial aging; the rest were unscreened new units. The high voltage applied to the SEM's was held constant at 3500 volts and they were operated as two-terminal devices, the charge collection electrode biased at 200 volts above the SEM operating voltage. The charge sensitive preamplifier outputs, were time multiplexed in an analog multiplexer and fed into a pulse height analyzer with 128 channel resolution, while a pulse rate counter measured and recorded the individual count rates of each SEM. The pulse rate counter threshold was 5×10^{-14} coulombs, which ensured that all output pulses were counted, regardless of amplitude. A digital control system provided the timing and sequencing functions, as well as the data printout. Initially, the SEM's exhibited a broad peak in the pulse height distribution, as specified by the manufacturer for two-terminal and gain saturated mode of operation, but after approximately 2×10^9 counts, the peak had virtually disappeared and the pulse height distribution was exponential in form,

indicating unsaturated operation. The results presented are for the average gain, that is the average number of output electrons per primary incident particle, computed from such exponential distribution. To deduce the average gain, the "center of gravity" of the distribution is calculated by numerical computation of the first moment and total area. The curves of Figures 9 and 10 show the variation of the average gain versus the total number of counts accumulated, for five of the six test units. Figure 11 shows the observed behavior of the pulse height distribution, as a function of operating voltage and accumulated counts. Unit number 5 is the flight assembly; the data for unit number 6 was extremely erratic and noisy due to problems in the preamplifier and therefore is not presented.

Although the plateau gains are lower than expected for some units, on the average they are satisfactory for the indicated charge threshold sensitivity of 5×10^{-14} coulombs, and the desired lifetime of one year. The initial gains varied between 3.5×10^{8} and 1×10^{8} and were not related to the final plateau gain.

The system had to be let up to atmospheric pressure on two occasions due to failures in the preamplifiers caused by corona discharge. In each case, after pump down and turn-on, the gain was observed to recover to a large fraction of the initial gain of the units, but decreased to the plateau level after 3 or 4×10^{9} counts.

It can be observed from the curves, that the onset of the gain fatigue region occurred at about 2.5×10^{10} counts. This is sooner than expected for SEM's on the basis of the published data and recent tests conducted by the manufacturer on similar units. Klettke et al.[18] and Graves[21], report the onset of the gain fatigue region to occur at

about 5 to $8x10^{10}$ counts, with a smaller slope than the one observed by us. However, their tests were performed at $3x10^{-11}$ torr and $1x10^{-7}$ torr respectively, and much higher operating voltages which ensured saturated mode operation; this is not our case as mentioned earlier. At approximately 10^{11} counts, the high voltage was raised to 4000 volts to simulate actual operating conditions in the spacecraft, and the results are shown as the dotted line in Figures 9 and 10. In general, the results of our tests confirm the reported characteristic behavior of electron channel multipliers, except for the earlier change of the shape of the pulse height distribution. Our primary objective was to determine whether the same conclusions obtained for curved channel multipliers could be applied to SEM's and thus estimate reliably the life expectancy of our instrument. This appears to be generally true, but with some reservations. It is clear that additional testing is required to fully understand and predict the observed behavior of these devices.

REFERENCES

1) M. Neugebauer, C. W. Snyder, Jet Propulsion Lab. Tech. Memo. 33-111, November 15, 1962.

2) J. H. Wolfe, R. W. Silva and M. A. Myers, "Observation of the Solar Wind During the Flight of IMP-1", J. Geophys. Res., 71, 1319, 1966.

3) A. J. Hundhausen, J. R. Asbridge, S. J. Bame, H. E. Gilbert and I. B. Strong,"Vela 3 Satellite Observations of Solar Wind Ions" - A Preliminary Report, J. Geophys. Res., 72, 87, 1967.

4) D. L. Lind and N. McIlwraith, "Plasma Electron Detector Using an Open Electron Multiplier", IEEE Transactions on Nuclear Science, 13, 511, 1966.

5) D. E. Robbins, A. J. Hundhausen and S. J. Bame, "Helium in the Solar Wind", J. Geophys. Res., 75, 1178, 1970.

5a) S. J. Bame et. al. "Solar Wind Ions" J. Geophys. Res., 75, 1178 1970.

6) K. W. Ogilvie, L. F. Burlaga and T. D. Wilkerson, "Plasma Observations on Explorer 34", J. Geophys. Res., 72, 6809, 1968.

6a) K. W. Ogilvie and T. D. Wilkerson, "Helium Abundance in the Solar Wind", Solar Physics, 8, 435, 1969.

7) J. A. Hirschberg, A. Alskne, D. S. Colburn, S. J. Bame and A. J. Hundhausen, "Observations of a Solar Flare Induced Interplanetary Shock and Helium Enriched Driver Gas", J. Geophys. Res., 75, 1, 1970.

8) W. H. Tucker and R. J. Gould, "Radiation from a Low Density Plasma at 10^{6° - 10^{8° K", Ap. J., 144, 244, 1966.

9) J. Geiss, "On Elemental and Isotopic Abundances in the Solar Wind", Asilomar Conference on the Solar Wind, 1971.

10) K. W. Ogilvie and T. D. Wilkerson, "Mass-Energy Spectrometer for Space Plasmas", Rev. Sci. Inst. 319, 441, 1968.

11) K. W. Ogilvie, R. I. Kittredge, T. D. Wilkerson, "Crossed-field Velocity Selector" Rev. Sci. Inst. 39, 459, 1968.

12) L. Wahlin, "The Colutron, A Zero Deflection Isotope Separator", Nuclear Inst. and Meth., 27, 55, 1964.

13) L. Wahlin, "The Colutron Mark II, A velocity Filter Isotope Separator", Nuclear Inst. and Meth., 38, 133, 1965.

14) C. N. Burrous, A. J. Lieber and V. T. Zavientseff, "Detection Efficiency of a Continuous Channel Electron Multiplier for Positive Ions", Rev. Sci. Inst., 38, 1477, 1967.

15) A. Egidi, R. Marconero, G. Pizzella and F. Sperli, "Channeltron Fatigue and Efficiency for Protons and Electrons", Rev. Sci. Inst., 40, 90, 1969.

16) M. C. Johnson, "A Secondary Standard Vacuum Ultraviolet Detector", Rev. Sci. Inst., 40, 311, 1969.

17) A. J. Hundhausen, "Composition and Dynamics of the Solar Wind Plasma", Rev. Geophys. Space Phys., 8, 729, 1970.

18) B. D. Klettke, N. D. Krym, W. G. Welber, "Long Term Stability Characteristics of Commonly Used Channel Electron Multipliers", Proc. Sixteenth Nuclear Science Symposium, IEEE, 1969.

19) R. D. Reed, E. G. Shelley, J. C. Backe, T. C. Sanders and J. D. McDaniel, "A Low Energy Channel Multiplier Spectrometer for ATS-E", IEEE Transactions on Nuclear Science, NS16, 359, 1969.

20) S. Cantarano, A. Egidi, R. Marconero, G. Pizzella and F. Sperli, "Effects of Fatigue in Channeltron Electron Multipliers", La Ricerca Scientifica, 37, 387, 1967.

21) P. Graves, Private communication.

FIGURE CAPTIONS

Figure 1 — IMP-H ion composition experiment

Figure 2 — Schematic representation of the ion optics section

Figure 3 — a) Measurement scheme. The 30 steps cover the range of 300 to 6500 eV/Z

b) Typical mass resolution curve for 960 eV ions. Here Vc is held constant and Vm varied over the voltage range shown.

Figure 4 — Limiting particle trajectories for the ion optics section. Each SEM has a 5.5^{o} field of view. Note the overlap of the SEM's fields of view. This ensures that there are no dead zones over the solid acceptance angle of the instrument.

Figure 5 — Spiraltron* detector assembly.

Figure 6 — Schematic diagram of the calibration system. The experiment platform has two degrees of freedom indicated by the arrows.

Figure 7 — Azimuthal angular response curves for 3 sets of values of Vc and Vm corresponding to the indicated steps.

Figure 8 — Elevation angular response characteristics.

Figure 9, Figure 10 — Variation of SEM's gain vs. total number of accumulated counts.

Figure 11 — SEM pulse height distribution vs. accumulated counts and operating voltage.

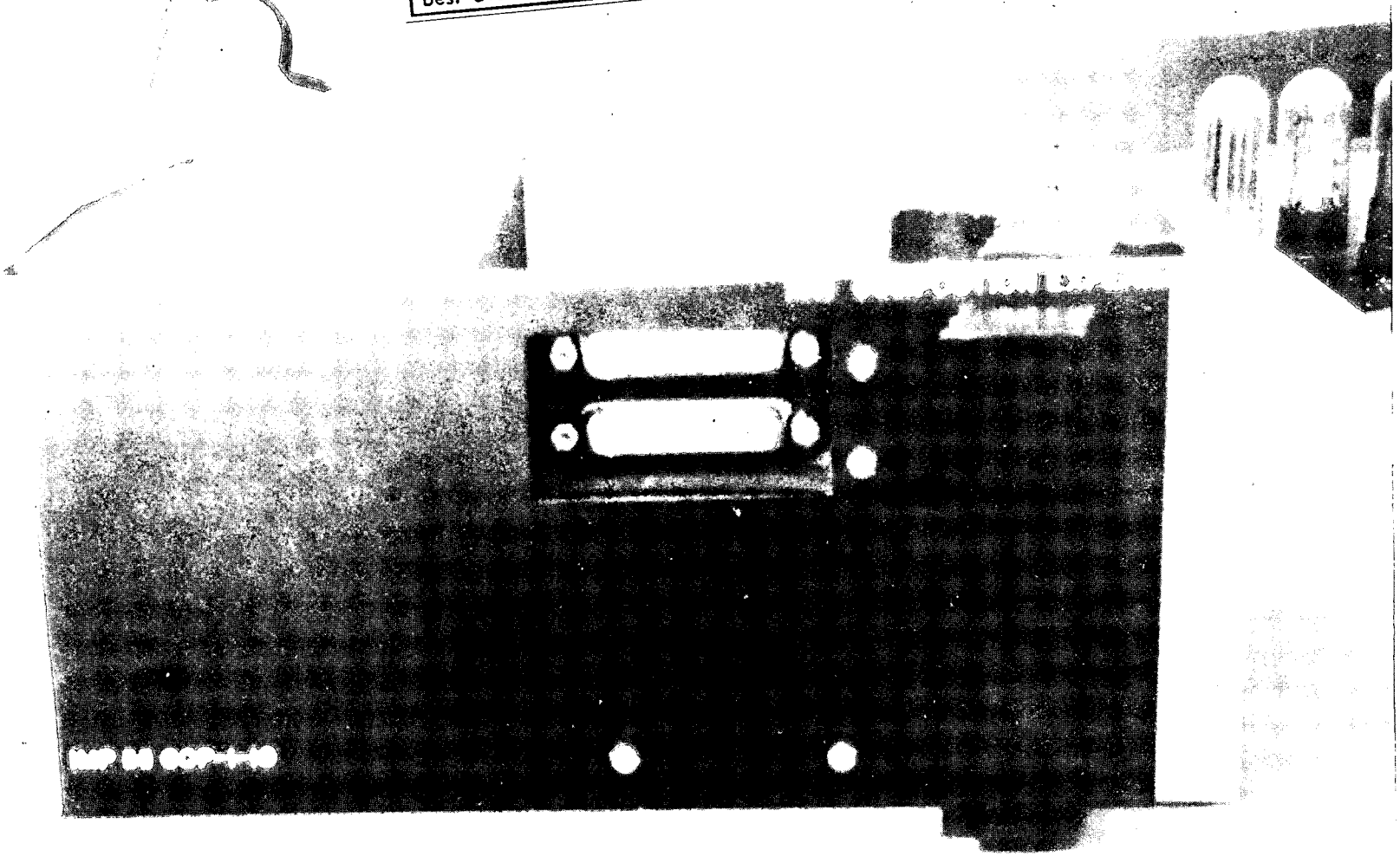

Figure 1

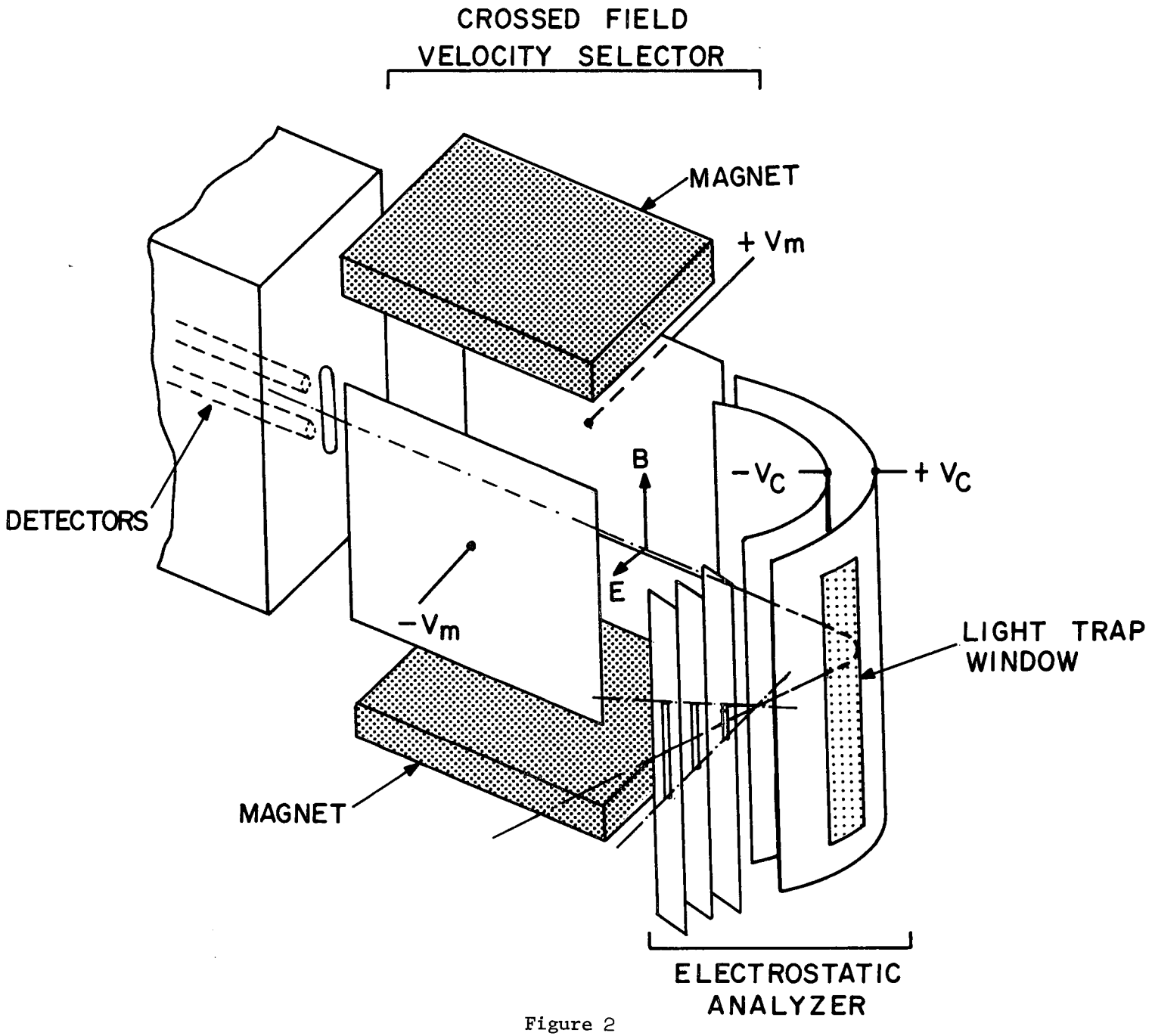
CROSSED FIELD
VELOCITY SELECTOR
MAGNET
+ Vm
DETECTORS
B
−Vc
+ Vc
E
−Vm
LIGHT TRAP
WINDOW
MAGNET
ELECTROSTATIC
ANALYZER

Figure 2

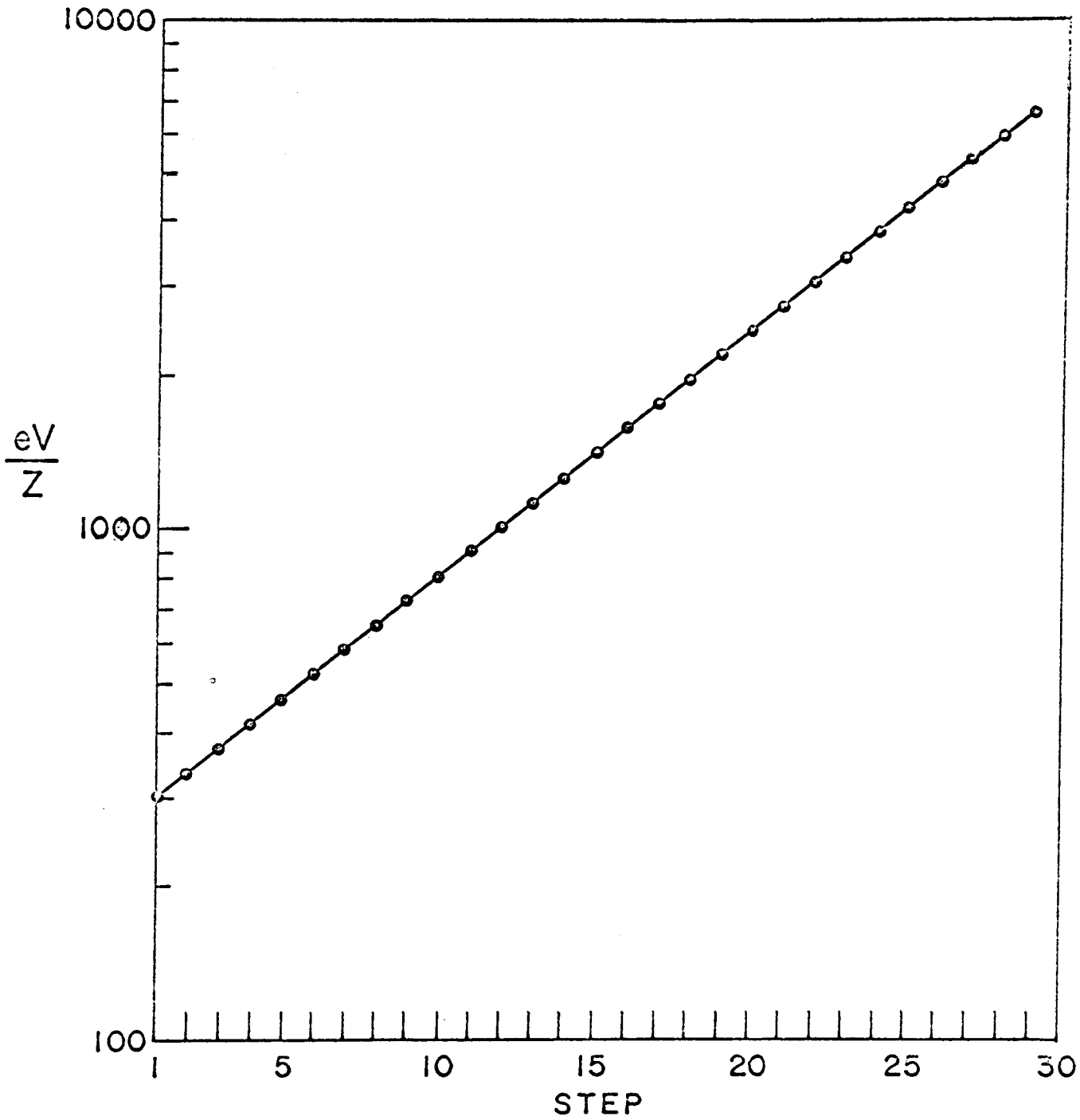

Figure 3

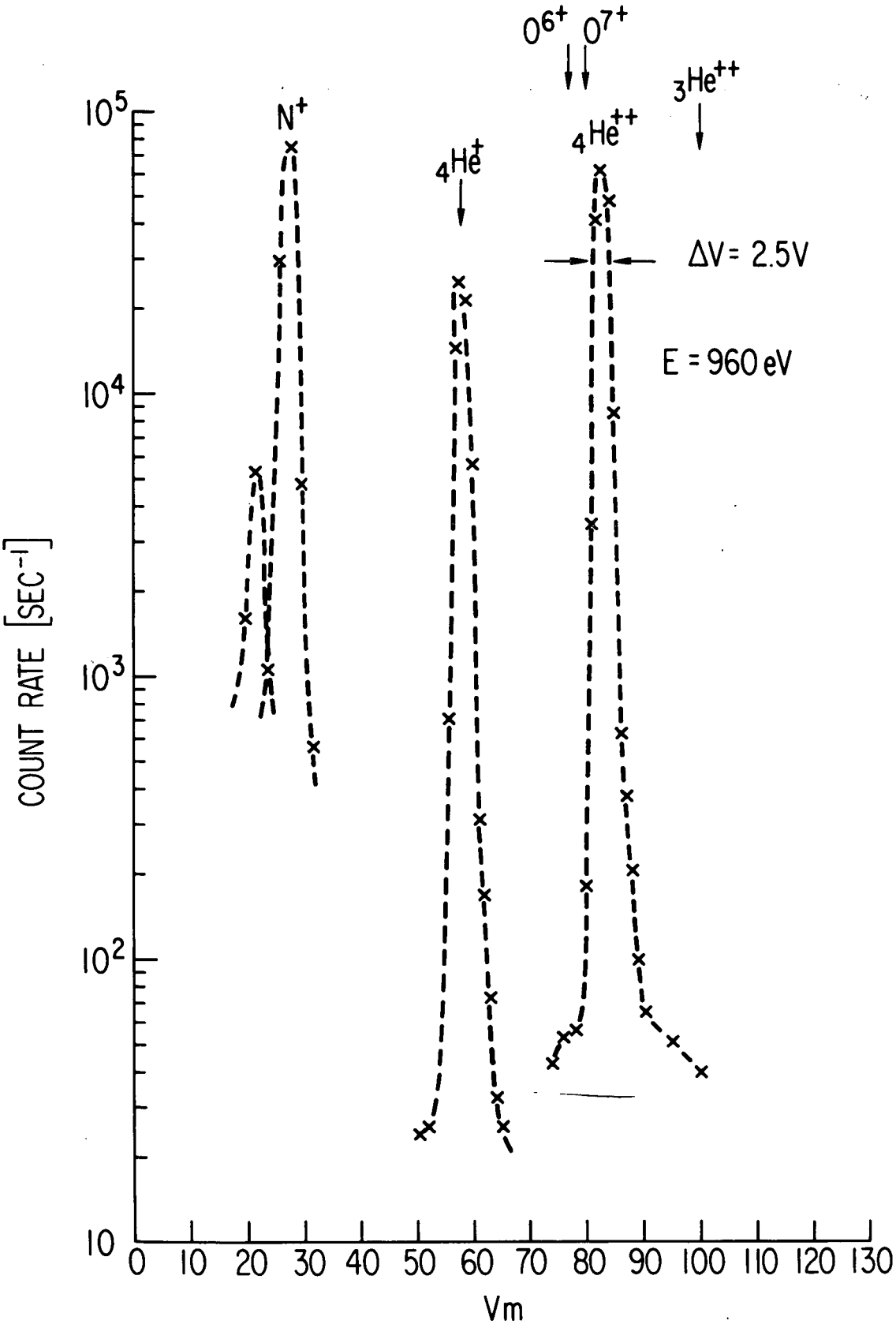
O^{6+} O^{7+}
$^3He^{++}$
$^4He^{++}$
$^4He^+$
N^+
ΔV = 2.5V
E = 960 eV
COUNT RATE [SEC^{-1}]
10^5
10^4
10^3
10^2
10
0 10 20 30 40 50 60 70 80 90 100 110 120 130
Vm

Figure 3b

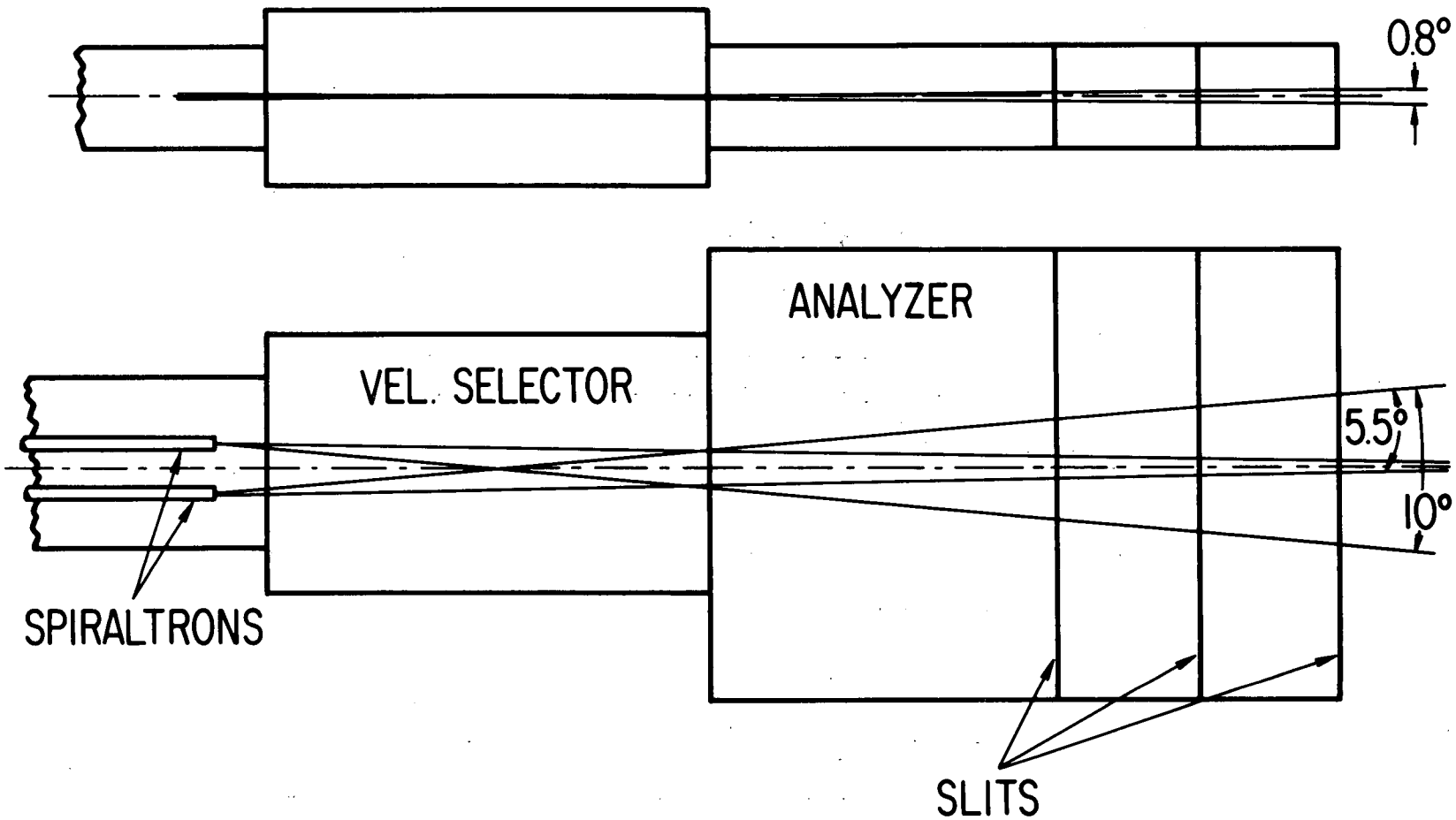

Figure 4

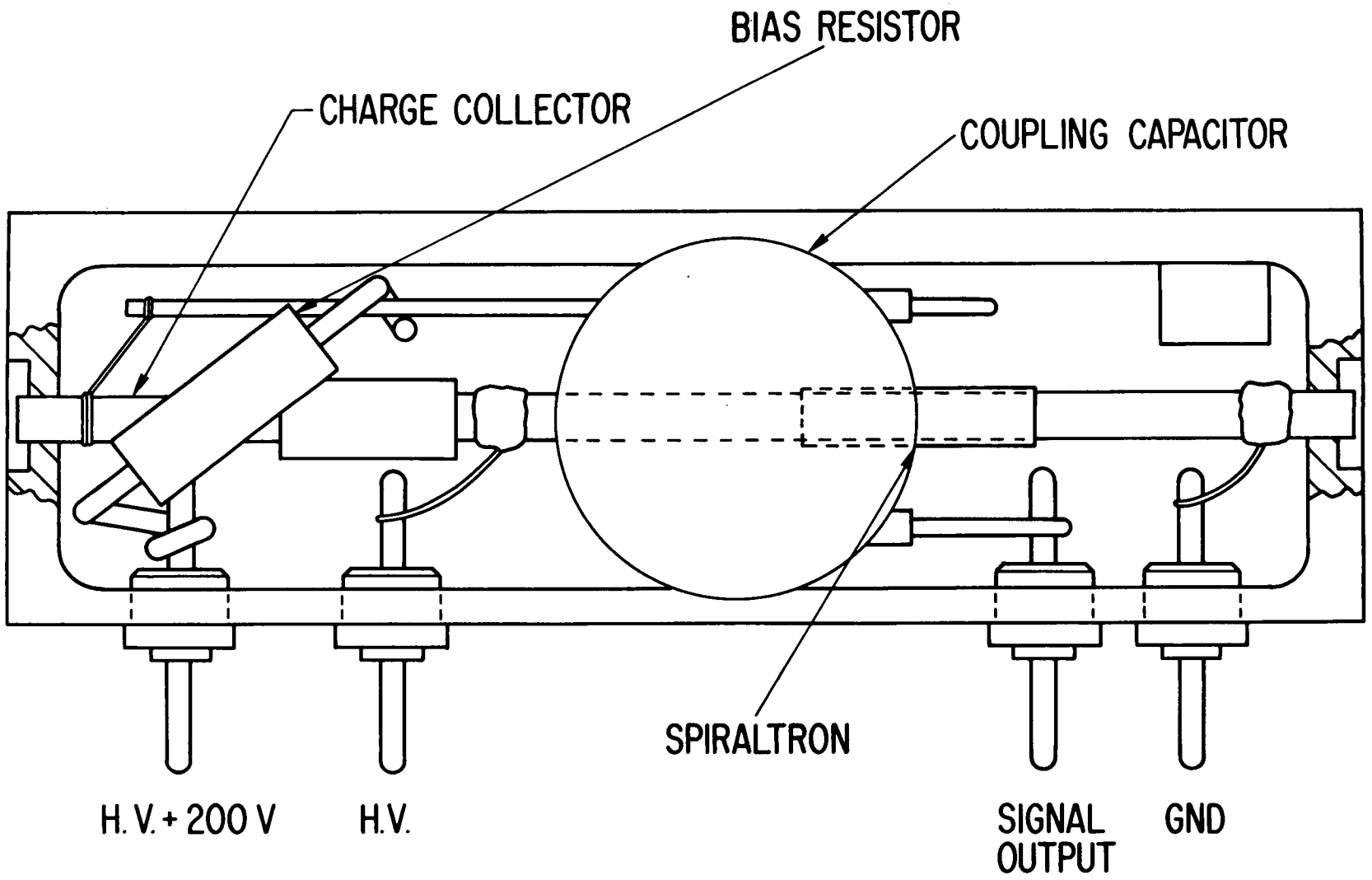
BIAS RESISTOR
CHARGE COLLECTOR
COUPLING CAPACITOR
SPIRALTRON
H.V. + 200 V
H.V.
SIGNAL OUTPUT
GND

Figure 5

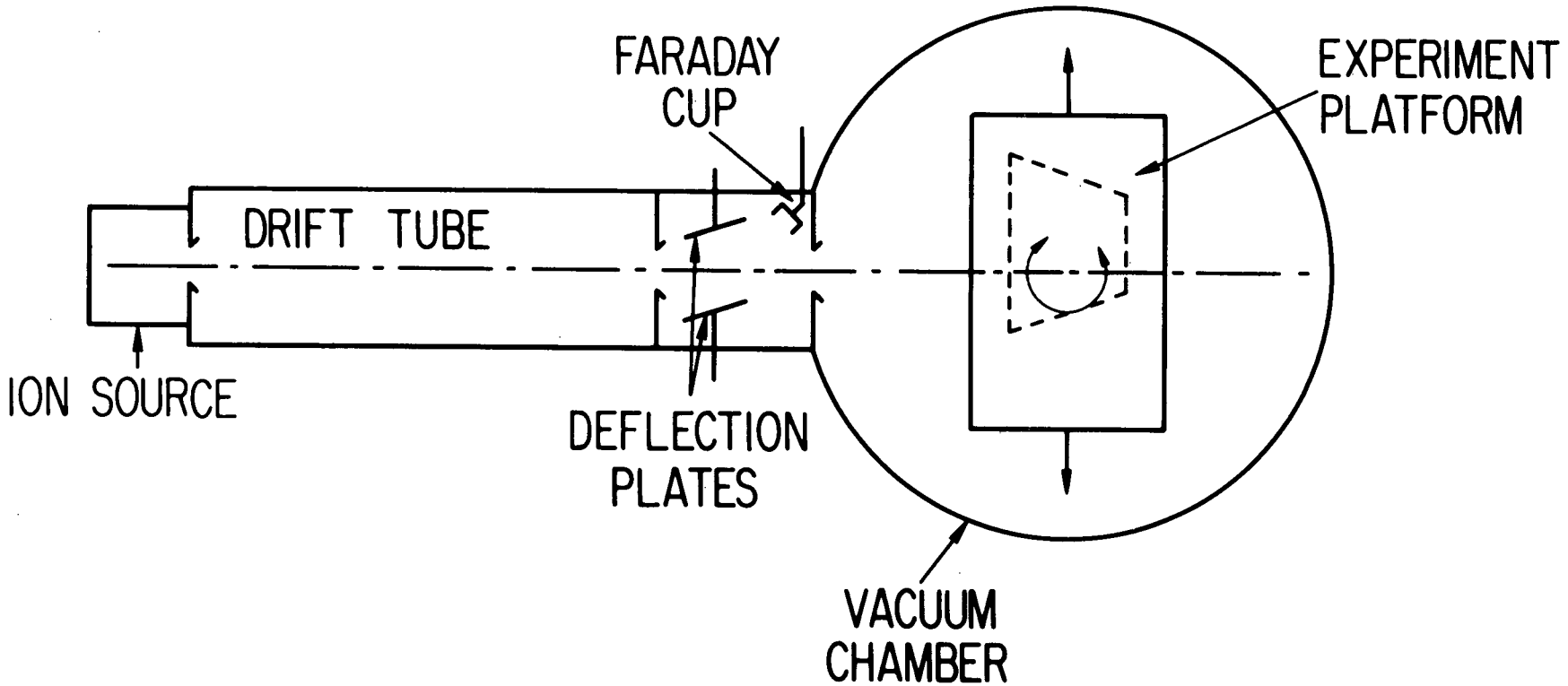
FARADAY
CUP
EXPERIMENT
PLATFORM
DRIFT TUBE
ION SOURCE
DEFLECTION
PLATES
VACUUM
CHAMBER

Figure 6

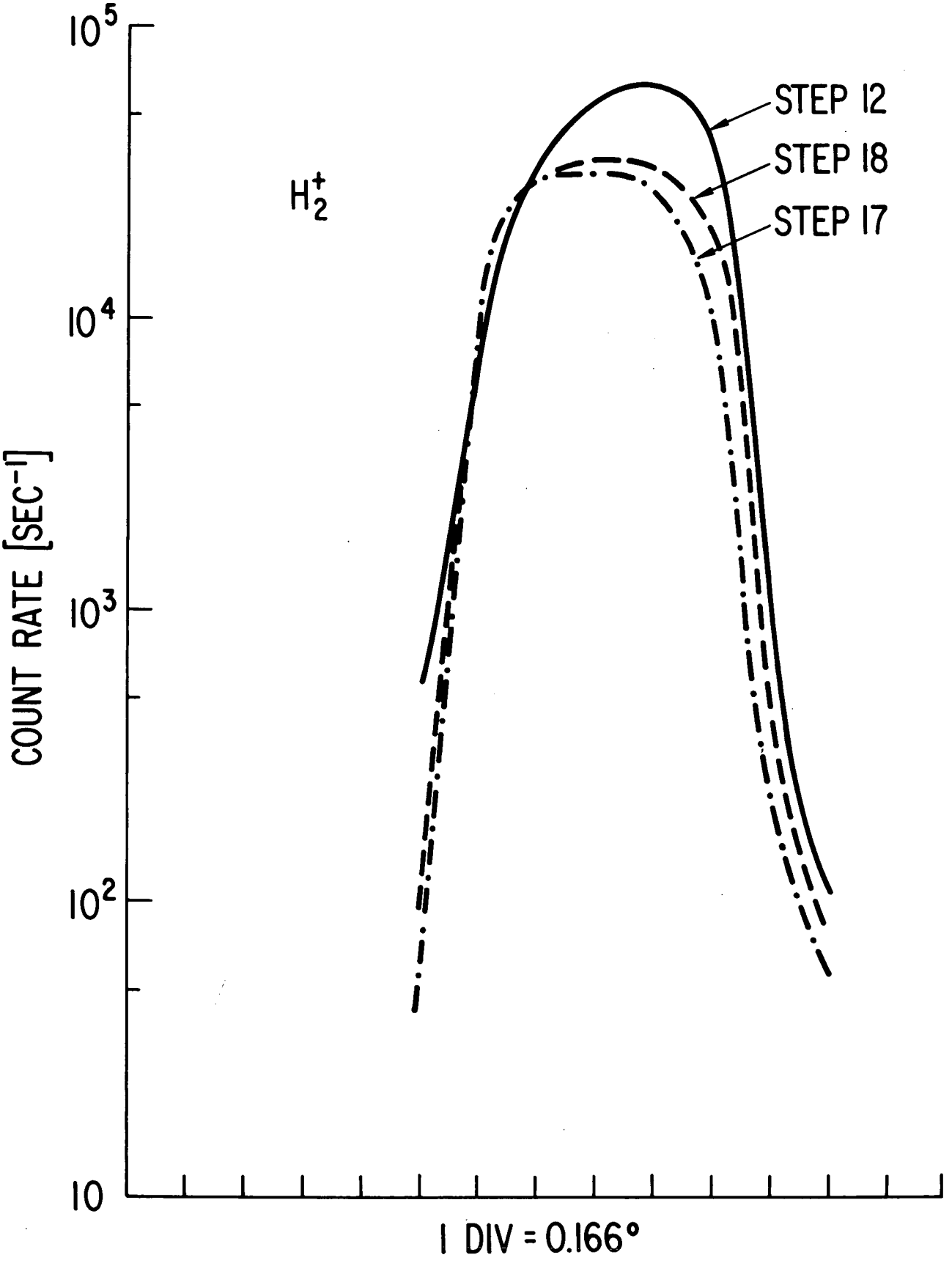
10^5
10^4
10^3
10^2
10
COUNT RATE [SEC^{-1}]
H_2^+
STEP 12
STEP 18
STEP 17
1 DIV = 0.166°

Figure 7

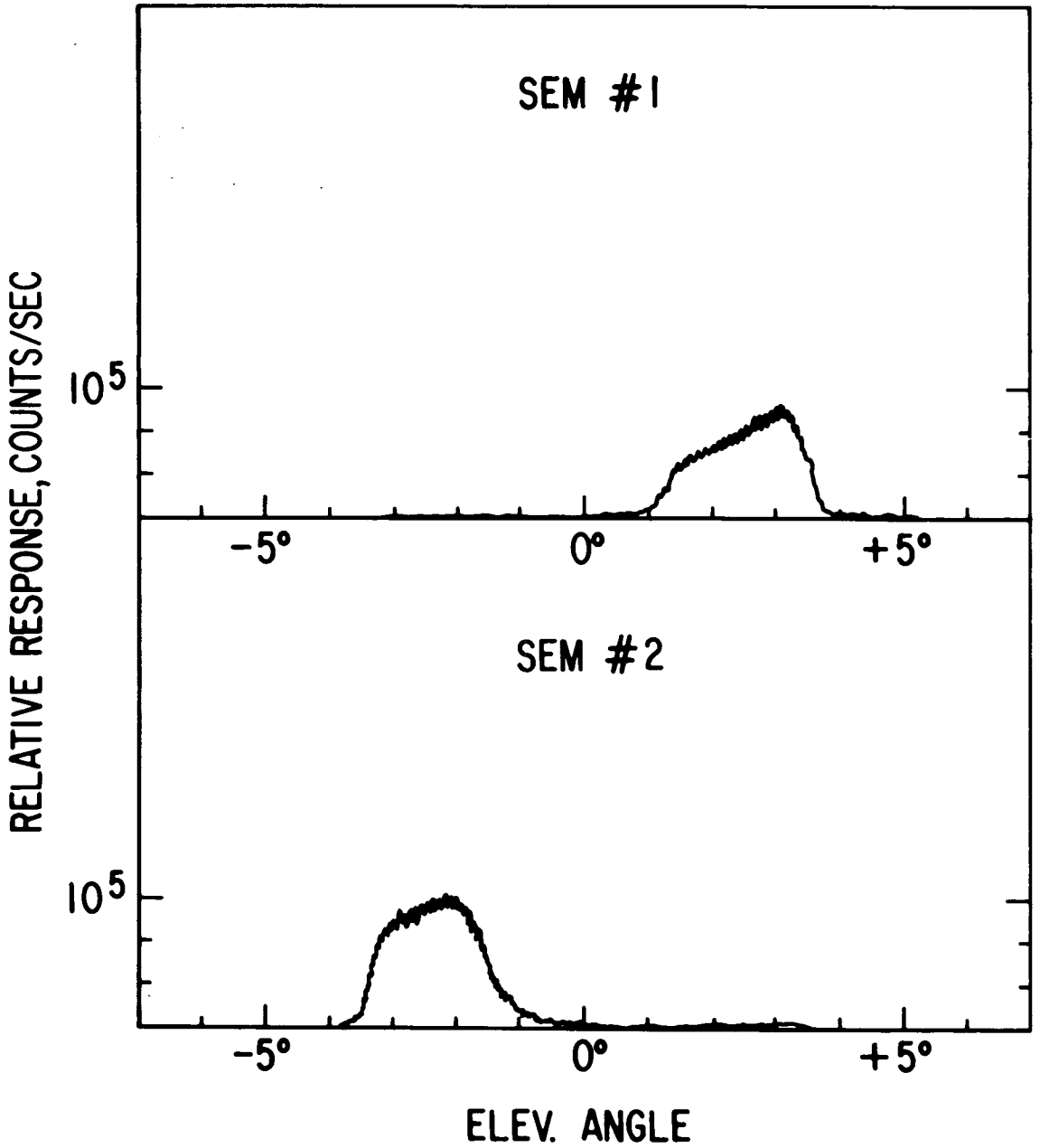
SEM #1
SEM #2
RELATIVE RESPONSE, COUNTS/SEC
10^5
10^5
-5°
0°
+5°
-5°
0°
+5°
ELEV. ANGLE

Figure 8

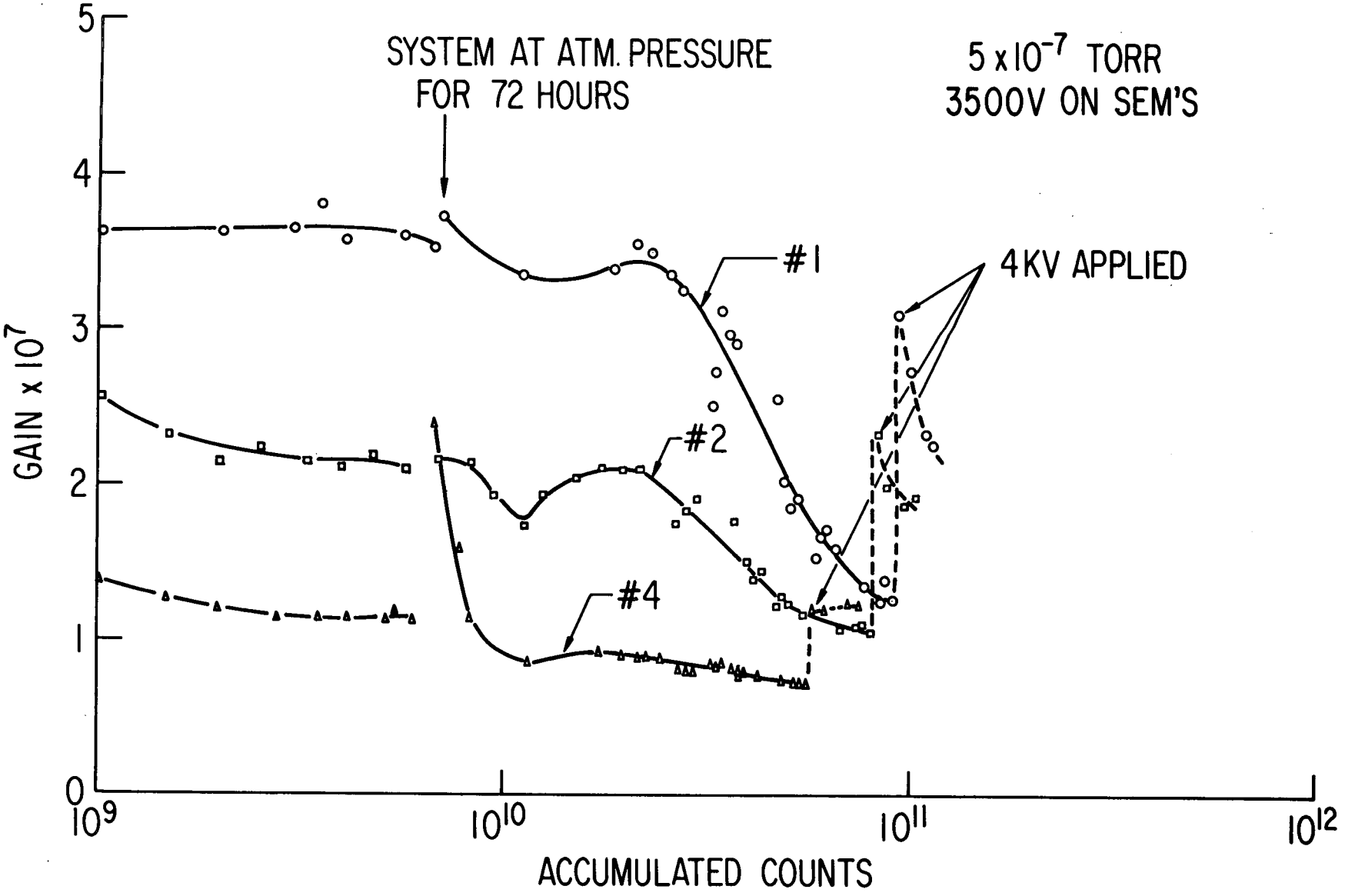
SYSTEM AT ATM. PRESSURE
FOR 72 HOURS
5 x 10⁻⁷ TORR
3500V ON SEM'S
#1
4KV APPLIED
#2
#4
GAIN x 10⁷
ACCUMULATED COUNTS
0
1
2
3
4
5
10⁹
10¹⁰
10¹¹
10¹²

Figure 9

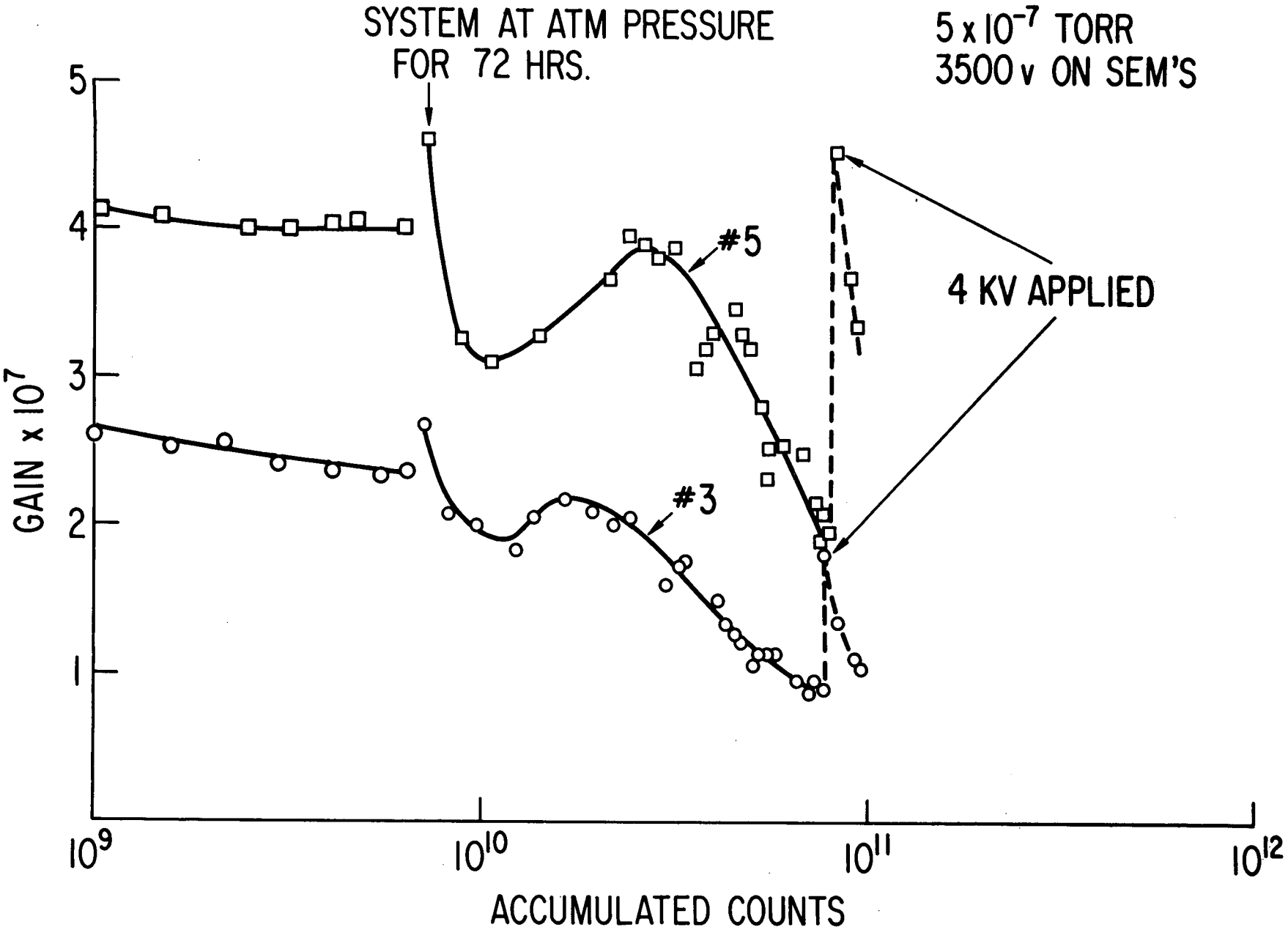
SYSTEM AT ATM PRESSURE
FOR 72 HRS.
5 x 10⁻⁷ TORR
3500 v ON SEM'S
4 KV APPLIED
#5
#3
GAIN x 10⁷
5
4
3
2
1
10⁹
10¹⁰
10¹¹
10¹²
ACCUMULATED COUNTS

Figure 10

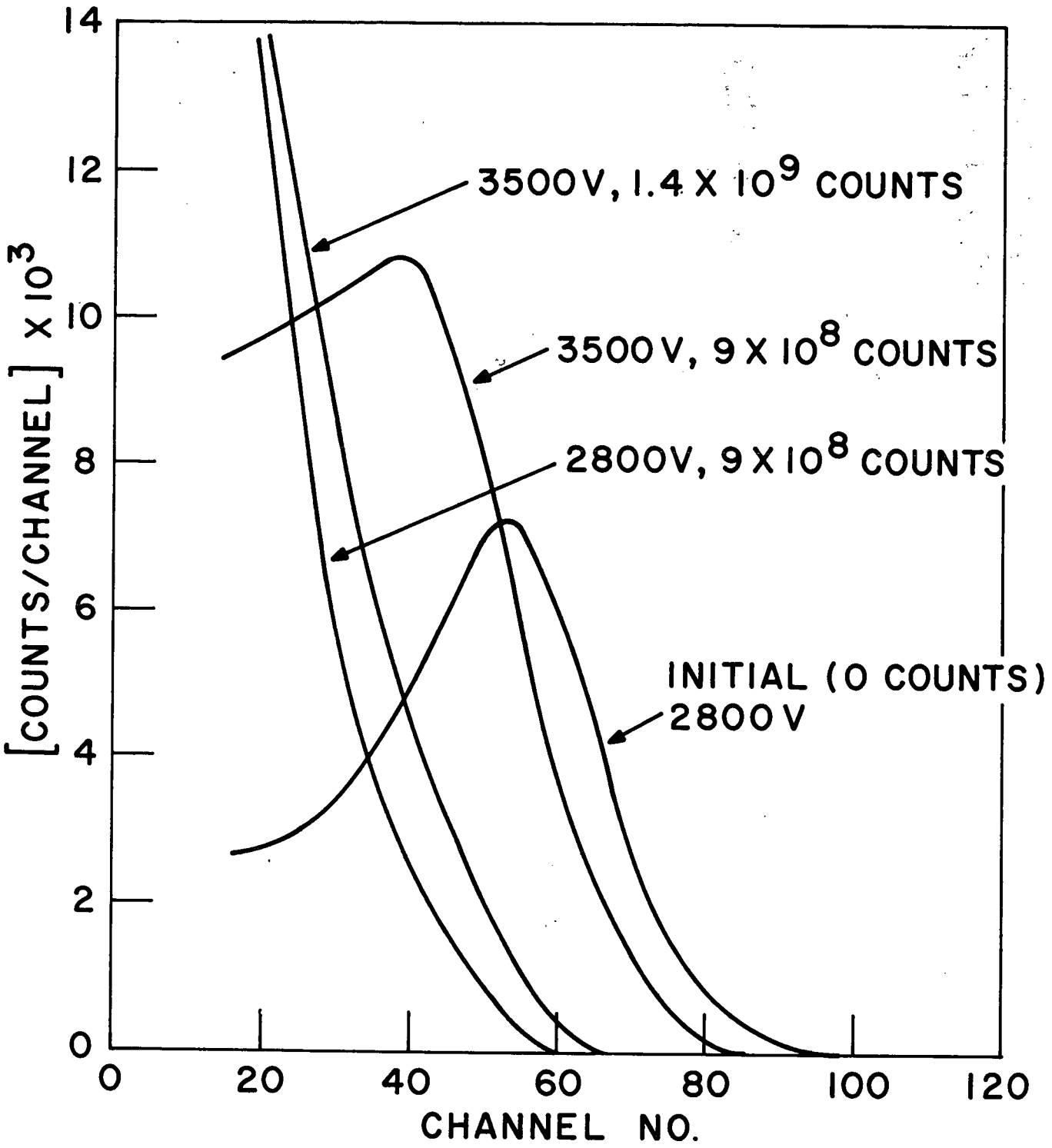
14
12
10
8
6
4
2
0
[COUNTS/CHANNEL] X 10^3
3500V, 1.4 X 10^9 COUNTS
3500V, 9 X 10^8 COUNTS
2800V, 9 X 10^8 COUNTS
INITIAL (0 COUNTS)
2800V
0
20
40
60
80
100
120
CHANNEL NO.

Figure 11